NF-κB2 is required for the establishment of central tolerance through an Aire-dependent pathway

Mingzhao Zhu,[1] Robert K. Chin,[1] Peter A. Christiansen,[1] James C. Lo,[1] Xiaojuan Liu,[1] Carl Ware,[2] Ulrich Siebenlist,[3] and Yang-Xin Fu[1]

[1]Department of Pathology and Committee on Immunology, University of Chicago, Chicago, Illinois, USA. [2]Division of Molecular Immunology, La Jolla Institute for Allergy and Immunology, San Diego, California, USA. [3]Immune Activation Section, Laboratory of Immune Regulation, National Institute of Allergy and Infectious Diseases, NIH, Bethesda, Maryland, USA.

NF-κB2–deficient mice have impaired T and B cell responses. We found, however, that in these mice there was severe infiltration of lymphocytes into multiple organs and increased activity of autoantibodies to peripheral tissue antigens in a manner similar to that of autoimmune regulator–deficient (Aire-deficient) mice. We further demonstrated that NF-κB2 was required for thymic *Aire* gene transcriptional regulation. The *Nfkb2*$^{-/-}$ thymus had distinct cortical and medullar structures, but reduced *Aire* and target gene expression of peripheral tissue antigens. Engraftment of *Nfkb2*$^{-/-}$ thymic stroma to nude mice recapitulated the autoimmune phenotype of the native *Nfkb2*$^{-/-}$ mice, confirming a key defect in central tolerance. Lymphotoxin β receptor (LTβR) ligation–induced *Aire* gene expression was also largely abolished in the absence of NF-κB2. Thus NF-κB2 downstream of LTβR plays an important role in the regulation of central tolerance in an Aire-dependent manner.

Introduction

Self tolerance is a fundamental property of the immune system. Thymic negative selection provides a critical mechanism for establishing self tolerance by eliminating the self-reactive T cell repertoire. How autoreactive T cells specific for peripheral tissue-specific antigens (TSAs) are purged from the thymus had been debated until recent evidence emerged demonstrating that TSAs are ectopically expressed in the thymus, specifically on medullary epithelial cells (1, 2). Autoimmune regulator (AIRE) is a recently discovered transcription factor that coordinates the expression of a set of TSAs in medullary thymic epithelial cells (mTECs) for the depletion of self-reactive T cells. The absence of thymic Aire expression leads to the escape of autoreactive T cells and results in frank autoimmunity (3, 4). With the understanding of AIRE's role in controlling promiscuous expression of TSAs and central tolerance, much interest has focused on how AIRE is regulated. Several molecules including lymphotoxin β receptor (LTβR), NF-κB–inducing kinase (NIK), and TNF receptor–associated factor 6 (TRAF-6) (5–8) have been implicated, as their respective deficient mice present similarly with increased multiorgan infiltration and autoantibody reactivity to peripheral antigens. How these findings are connected, however, remains elusive. TRAF-6, for example, is downstream of neither LTβR nor NIK. Yet TRAF-6–deficient mice have a disorganized thymic structure similar to that of NIK$^{aly/aly}$ mice, a natural strain with alymphoplasia caused by a point mutation in the gene encoding NIK (5, 9). On the other hand, despite being upstream of NIK, LTβR-deficient mice show thymic architec-

ture similar to that of WT mice (7, 10). Therefore, NIK may receive additional signals to regulate thymic architecture while TRAF-6 lies in a different signaling pathway to control central tolerance.

NF-κB2 transduces signals downstream of both LTβR and NIK. While both LTβR and NIK are critical for secondary lymphoid organ organization and development, only NIK has an additional role in thymic architecture organization (9–12). *Ltbr*$^{-/-}$, NIK$^{aly/aly}$, and *Nfkb2*$^{-/-}$ mice all lack Peyer's patches, B cell follicles, and follicular DC networks (9–12). However, in contrast to *Ltbr*$^{-/-}$ and NIK$^{aly/aly}$ mice, *Nfkb2*$^{-/-}$ mice have milder microarchitectural changes in the spleen, retain almost all lymph nodes, and display normal thymic architecture (13, 14). These findings indicate that other downstream signaling pathways may also coordinate with the NF-κB2 pathway for secondary lymphoid organ development and organization (15). Therefore, the role of NF-κB2 in regulating central tolerance remains unclear.

Nfkb2$^{-/-}$ mice also present with reduced peripheral B cell populations and impaired B cell function (13, 14). In the T cell compartment, NF-κB2 appears to be important for T cell proliferation and resistance to apoptosis (16). In the absence of NF-κB2, mice infected with *Toxoplasma gondii* fail to maintain their T cell responses, due in part to increased apoptotic attrition (16). While these data suggest NF-κB2 to be an activator of the immune response, we were surprised to find that *Nfkb2*$^{-/-}$ mice harbored a strong autoimmune phenotype, implying that NF-κB2 may have a dominant role in self tolerance. Given that *Nfkb2*$^{-/-}$ mice present with a pattern of autoimmunity reminiscent of *Aire*$^{-/-}$ mice, we sought to determine whether NF-κB2 played an essential role in central tolerance. In this study, we found that NF-κB2 was necessary for thymic *Aire* gene transcriptional regulation. NF-κB2 deficiency in the thymic stroma was sufficient to lead to autoimmunity. Thus, NF-κB2 plays an important active role in establishing central tolerance through an Aire-dependent pathway.
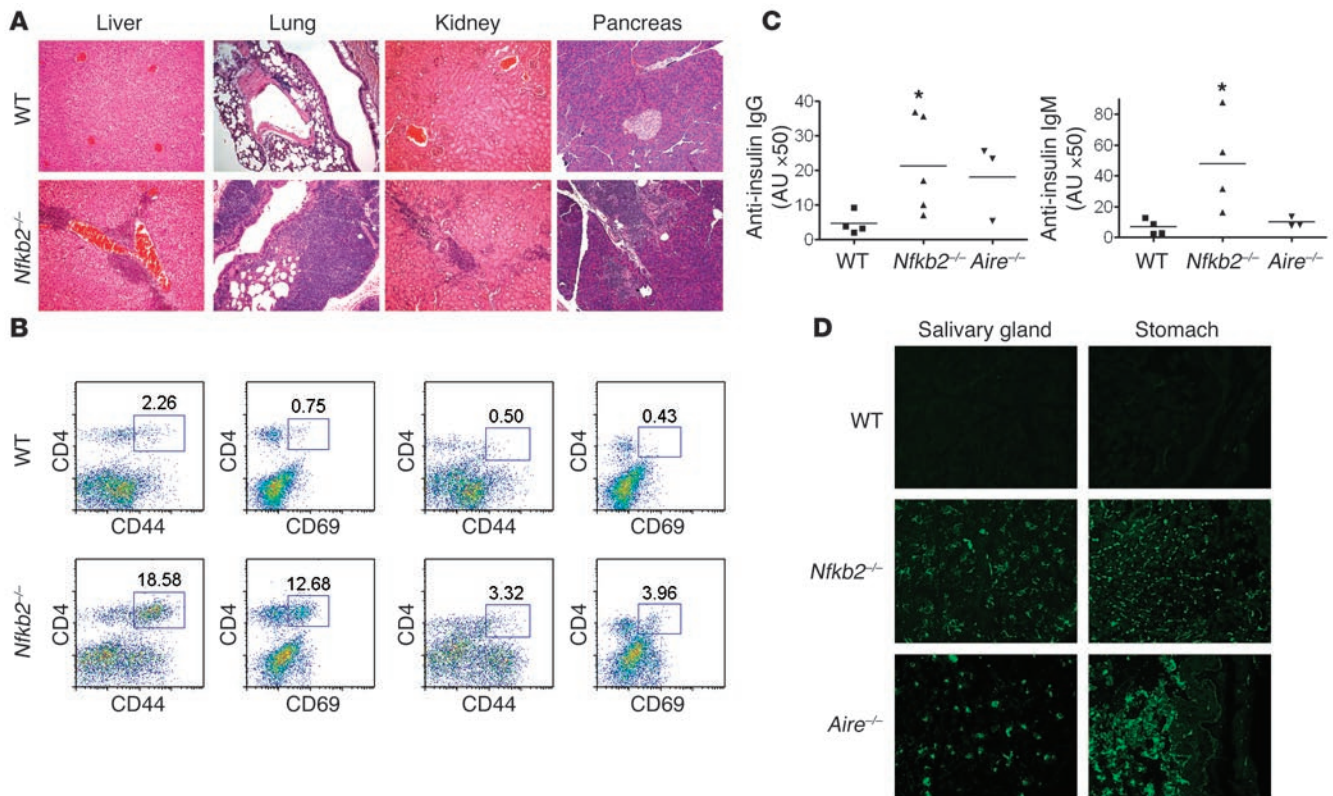
Figure 1
Autoimmunity in *Nfkb2*−/− mice. (**A**) H&E staining of formalin-fixed sections of livers, lungs, kidneys, and pancreata from 6- to 8-month-old WT or *Nfkb2*−/− mice. Magnification, ×200. (**B**) Increased percentage of activated and memory T cells in the lungs of 6- to 8-month-old *Nfkb2*−/− mice compared with age-matched WT mice. Numbers represent the percentages within the indicated regions. Data are representative of 3 experiments. (**C**) Increased levels of anti-insulin IgG and IgM were detected in 6- to 8-month-old *Nfkb2*−/− mice compared with age-matched WT mice. *P < 0.05 versus WT. (**D**) Autoantibodies were determined by immunofluorescence staining of *Rag1*−/− tissue sections. Magnification, ×100.

Results

Autoimmune phenotype in NF-κB2–deficient mice. NF-κB2 has been described to play an important role in developing optimal T and B cell responses (13, 14, 16). However, our analysis of *Nfkb2*−/− mice aged 6–8 months revealed marked lymphocytic infiltration of the livers, lungs, kidneys, and pancreata (Figure 1A). Such infiltrates were not seen in WT or *Nfkb1*−/− mice of similar age (data not shown). To confirm that this cellular infiltration is a result of an active, ongoing immune response rather than a passive displacement, infiltrating cells in the lung were isolated by collagenase digestion and then examined for lymphocyte activation and memory markers by flow cytometry analysis. Staining of activation marker CD69 demonstrated a 16-fold increase in the percentage of activated CD4 cells and a 9-fold increase in the percentage of activated CD8 cells in the lungs of *Nfkb2*−/− mice (Figure 1B). The percentage of the CD44+ memory cell population was increased by about 6- to 8-fold within CD4 and CD8 cells of *Nfkb2*−/− mice (Figure 1B). The increase of the percentage of both activated and memory cells, together with an approximately 3- to 4-fold increase in the absolute number of infiltrating lymphocytes, suggests that the infiltration in the lung is the result of an active, ongoing immune response.

To examine further whether self reactivity is manifested in *Nfkb2*−/− mice, 6-month-old *Nfkb2*−/− and WT mice were bled, and the autoreactive antibodies were tested by both ELISA and immunofluorescence staining of tissues from *Rag1*−/− mice. Sera from age-matched *Aire*−/− mice were used as a positive control. The ELISA results demonstrated significantly higher titers of both IgG and IgM autoantibodies to insulin in 6- to 8-month-old *Nfkb2*−/− mice relative to age-matched WT mice (Figure 1C). To test more generalized organ-specific autoimmunity, we detected autoreactive antibodies directed against salivary gland and stomach by immunofluorescence staining of *Rag1*−/− tissue sections in the sera of *Nfkb2*−/− mice and found them to be similar to those of *Aire*−/− mice, but not in WT mice (Figure 1D). These data indicate that NF-κB2 deficiency leads to autoimmunity.

Autoimmunity stems from a defect in the radiation-resistant stromal compartment. Since the NF-κB2 pathway plays important roles in both stromal and hematopoietic compartments, we next used BM chimeras to distinguish the contributions of each compartment to the autoimmune phenotype. Reciprocal transfers were performed with *Nfkb2*−/− BM transplanted into lethally irradiated WT mice, WT BM transplanted into *Nfkb2*−/− mice, and WT BM into WT mice as a control. At 12 weeks, examination of peripheral organs, including liver, lung, kidney, pancreas, salivary gland, and stomach, revealed no infiltration in WT hosts of WT BM and minor to no infiltration in WT hosts of *Nfkb2*−/− BM. In stark contrast, *Nfkb2*−/− recipients of WT BM presented with severe infiltrations in the liver and lung (Figure 2). This suggests that NF-κB2 deficiency in the radiation-
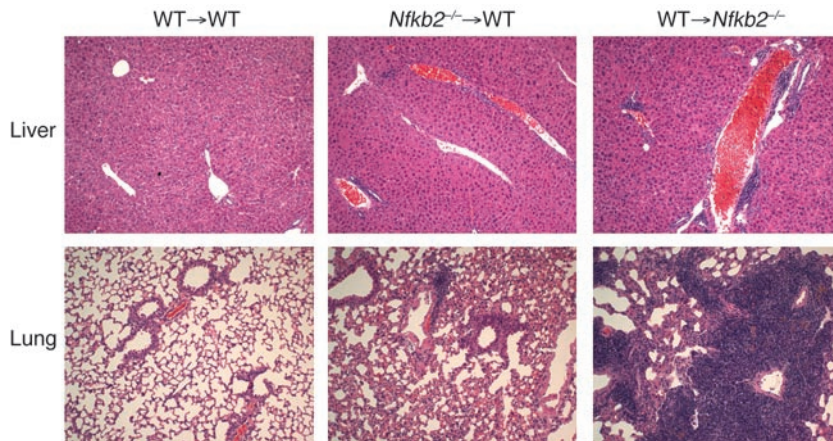
Figure 2
Autoimmunity in *Nfkb2*^{−/−} mice resulted from stroma defect. H&E staining of formalin-fixed sections of liver and lung from BM chimeras. Recipients were lethally irradiated, and 3×10^6 BM cells were transplanted i.v. H&E staining was performed 12 weeks after BM reconstitution. Magnification, ×200.

resistant stroma, rather than the hematopoietic compartment, is the primary cause of the witnessed autoimmunity.

Central defect of reduced expression of Aire and other TSA genes in Nfkb2^{−/−} *mice.* Due to the similarity in autoimmune phenotypes among *Nfkb2*^{−/−} and *Aire*^{−/−}, *Ltbr*^{−/−}, *Traf6*^{−/−}, and NIK[aly/aly] mice, we wondered whether NF-κB2 deficiency results in a defect in mTEC expression of *Aire*, a critical step for eliminating autoreactive thymocytes and establishing central self tolerance. To explore whether *Nfkb2*^{−/−} mice harbor a defect in mTEC development, thymi from 5- to 7-week-old *Nfkb2*^{−/−} and WT mice were first analyzed by H&E staining. The *Nfkb2*^{−/−} thymi were well developed and organized, with similar size to and distinct medullary and cortical areas as in WT thymi. Although the medulla was a little more isolated in *Nfkb2*^{−/−} than that in WT thymi, by calculating the areas of the medulla and cortex, we found no significant difference in terms of the ratio of medulla to cortex compared with WT thymus (WT, 0.35 ± 0.08; *Nfkb2*^{−/−}, 0.30 ± 0.09; *P* = 0.49; Figure 3A). Next we specifically visualized mTECs by immunofluorescence staining of different medulla markers. We used antibodies to epithelial cell adhesion molecule (Ep-CAM; also referred to as G8.8), which has been reported to recognize most mTECs (17), and *Ulex europaeus* agglutinin 1 (UEA-1), a lectin that binds to mature mTECs (18). Representative staining results are shown in Figure 3B. Further quantitative analysis revealed somewhat reduced numbers of G8.8[+] and UEA-1^{+} cells in *Nfkb2*^{−/−} thymi compared with WT (Figure 3C). This suggests that NF-κB2 might play a role in the development and/or organization of mTECs. Aire is preferentially expressed in mTECs and drives the ectopic expression of a collection of peripheral TSAs such as insulin 1 (Ins1), casein α (Csna), and salivary protein 1 (Sp1) (3, 19, 20). To determine whether Aire expression was perturbed in *Nfkb2*^{−/−} thymi, the expression was first visualized by anti-Aire antibody. Significant reduction of Aire expression was found in *Nfkb2*^{−/−} thymi as well as in *Aire*^{−/−} thymi (Figure 3D). To further determine quantitatively the reduction of *Aire* expression and whether *Ins1*, *Csna*, and/or *Sp1* expression are also sufficiently impaired in *Nfkb2*^{−/−} thymi, we performed total thymus real-time PCR. We found about 3-fold reduced *Aire* expression and dramatically decreased *Ins1*, *Csna*, and *Sp1* gene expression in *Nfkb2*^{−/−} thymi compared

with age-matched WT thymi (Figure 3E). Similarly, *Ins2*, an important gene in the development of IDDM, is an another Aire-dependent TSA and was also found to be significantly reduced in *Nfkb2*^{−/−} thymi compared with WT (Supplemental Figure 1A; supplemental material available online with this article; doi:10.1172/JCI28326DS1). Since the mTEC population was found to be slightly reduced in *Nfkb2*^{−/−} thymi, to more specifically quantitate the role of NF-κB2 in transcriptional regulation of expression of *Aire* and other TSA genes within the mTEC population, we purified the mTECs (CD45^{−}G8.8^{+}B7.1^{+}) by fluorescence-activated cell sorting and reanalyzed *Aire*, *Ins1*, *Csna*, and *Sp1* gene expression with *Keratin 14* (*Krt14*) as a control. This keratin subset is constitutively and specifically expressed in the majority of mTECs in the thymus (21) and was not regulated by NF-κB2 (data not shown). Expression of *Aire*, *Ins1*, *Csna*, and *Sp1* was again reduced significantly in *Nfkb2*^{−/−} mTECs compared with WT mTECs on a per-cell basis (Figure 3F). *Ins2* was also detected at a lower level in *Nfkb2*^{−/−} mTECs compared with WT mTECs on a per-cell basis (Supplemental Figure 1B). It thus appears that NF-κB2 is required for optimal *Aire*, *Ins1*, *Csna*, and *Sp1* expression within mTECs. Aire is expressed not only in mTECs, but also in DCs, which suggests it might play additional roles other than TSA transcriptional regulation, such as T cell–APC interaction and APC-mediated T cell activation for self tolerance (22, 23). We therefore detected *Aire* expression in DCs. Interestingly, *Aire* expression in DCs appeared to also be regulated by NF-κB2, since a significant reduction was found in *Nfkb2*^{−/−} thymic DCs (Figure 3G) and splenic DCs (Figure 3H). This further supports the role of NF-κB2 for *Aire* transcriptional regulation in mTECs.

As DCs also serve as an important source of ectopic TSA expression in self tolerance (24–26), we further sought to determine whether these TSAs were expressed in thymic and splenic DCs, and if so, whether they were interrupted by a lack of NF-κB2. We did not detect *Ins1*, *Ins2*, *Csna*, or *Sp1* expression in purified thymic DCs by real-time PCR within 50 cycles (data not shown). This might indicate that DCs are not the major cell population for ectopic expression of *Ins1*, *Ins2*, *Csna*, and *Sp1* in the thymus. Whether some other TSAs are prominently expressed in thymic DCs and regulated by NF-κB2 remains to be determined. In the peripheral, *Ins1* and *Ins2*, but not *Csna* or *Sp1*, were readily detected in splenic DCs, although at much lower levels (about 30- and 200-fold for *Ins1* and *Ins2*, respectively) than in mTECs. Moreover, splenic DCs lacking NF-κB2 had significantly reduced *Ins1* and *Ins2* expression (Figure 3H and Supplemental Figure 1C). Thus, NF-κB2 appears to be required for optimal expression of *Aire* and other TSA genes not only within mTECs, but also in DCs.

No defect in the development of CD4^{+}*CD25*^{+} *Tregs.* CD4^{+}CD25^{+} Tregs generated in the thymus can actively suppress autoimmune responses, and their absence leads to severe autoimmunity (27–29). Since it has been reported that Treg generation in the thymus can be induced by the expression of self peptides within mTECs (30, 31), it is possible that the autoimmunity seen in *Nfkb2*^{−/−} mice could be due to defective thymic Treg generation. Foxp3 is presently the most definitive functional marker for Tregs (27–29). To determine wheth-
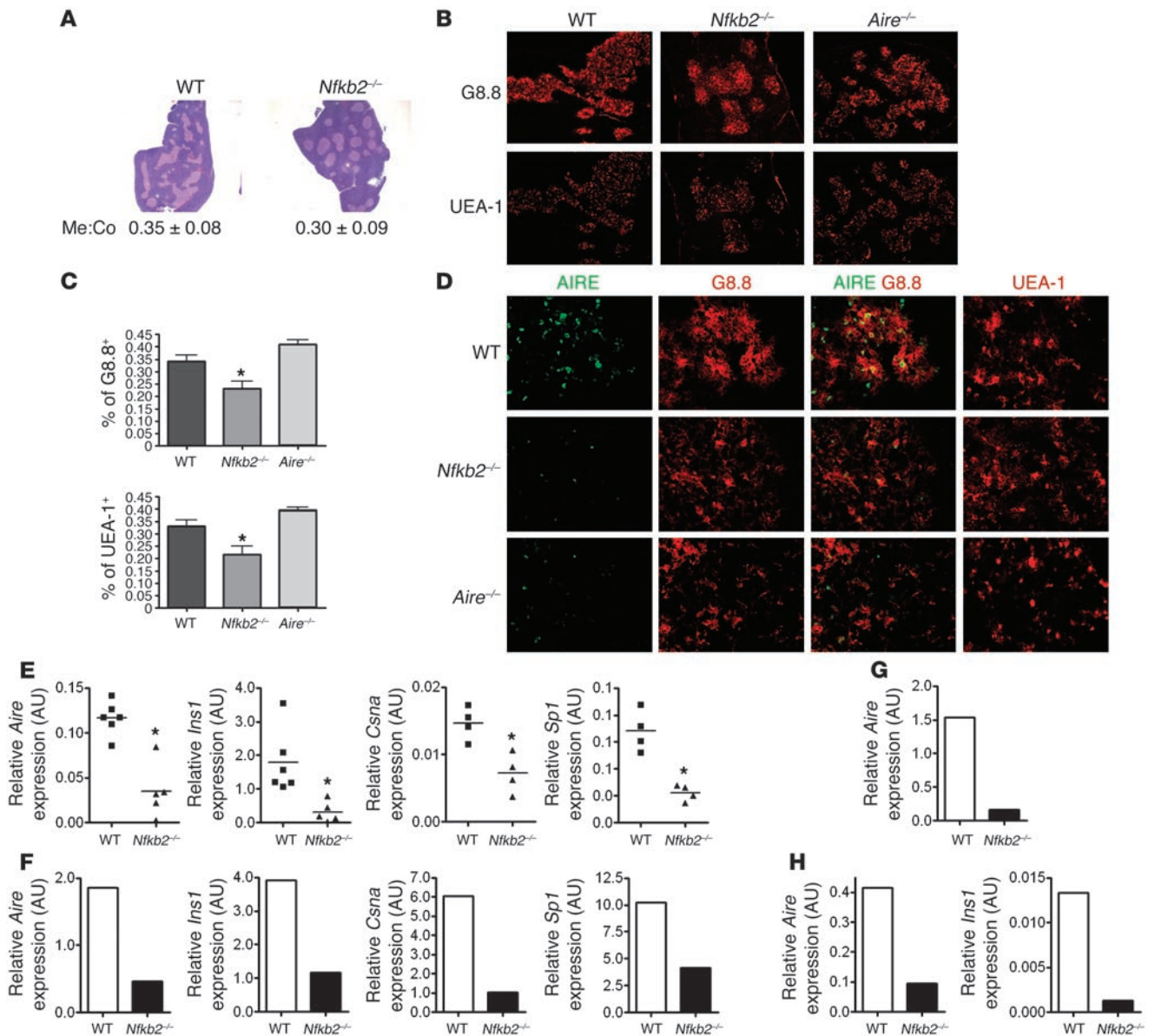
Figure 3
Thymic defect of reduced expression of *Aire* and other TSA genes in *Nfkb2−/−* mice. (**A**) H&E staining of 5- to 7-week-old *Nfkb2−/−* and WT thymi. Numbers indicate statistic mean ratio of medulla to cortex area (Me:Co) ± SEM from 4 different sections (*P* = 0.49). Magnification, ×12.5. (**B**) Immunofluorescence staining of 5- to 7-week-old *Nfkb2−/−* and WT thymi with anti–Ep-CAM (G8.8) and UEA-1. Magnification, ×40. (**C**) Quantitative analysis of the percentage of G8.8+ or UEA-1+ area from 4 digital fields. *P < 0.05 versus WT. (**D**) Aire expression in the thymic medullary area was reduced in the *Nfkb2−/−* thymus. G8.8+ and UEA-1+ (red) staining represent the majority of mTECs. Aire expression was visualized by FITC (green). Magnification, ×200. (**E**) Real-time PCR analysis of *Aire*, *Ins1*, *Csna*, and *Sp1* expression in 5- to 7-week-old *Nfkb2−/−* and WT thymi. Values are arbitrary units normalized to *Gapdh*. *P < 0.05 versus WT. (**F**) Real-time PCR analysis of *Aire*, *Ins1*, *Csna*, and *Sp1* expression from purified mTECs of 5- to 7-week-old *Nfkb2−/−* and WT thymi. Values are arbitrary units normalized to *Krt14*. Data are representative of 3 experiments. (**G** and **H**) Real-time PCR analysis of *Aire* expression in purified thymic DCs (**G**) or *Aire* and *Ins1* expression in purified splenic DCs (**H**). Values are arbitrary units normalized to *Gapdh*. Data are representative of 2 experiments.

er Treg generation in the thymus is impaired by NF-κB2 deficiency, thymic *Foxp3* gene expression was first analyzed by real-time PCR. We found no significant difference in *Foxp3* expression between *Nfkb2−/−* and WT thymi (Figure 4A). This finding was further confirmed by intracellular staining for Foxp3, which revealed no change in the percentage of Foxp3+CD4+ thymocytes (Figure 4B). We did not find any defect in the suppressive function of *Nfkb2−/−* CD4+CD25+

Tregs in the CD4+CD25− T cell proliferation assay upon anti-CD3 stimulation (data not shown). Thus, NF-κB2 deficiency does not lead to deficient thymic generation of CD4+CD25+ Tregs.

NF-κB2 in the thymic stroma is required for self tolerance. To demonstrate conclusively that the autoimmune phenotype in *Nfkb2−/−* mice is due to a defect in the thymic stroma, we performed thymus transplant experiments. Fetal thymi from *Nfkb2−/−* and WT mice
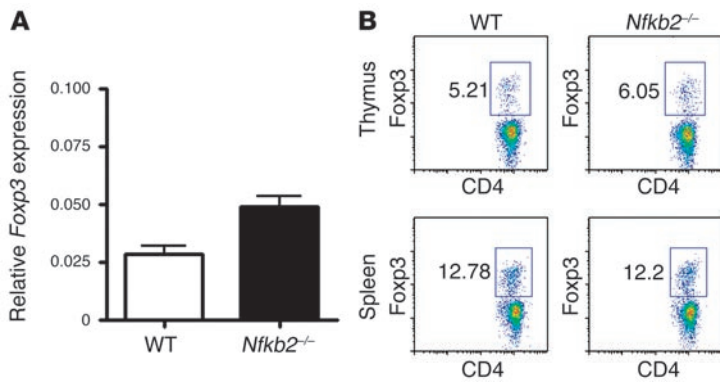
Figure 4
No defect of CD4+CD25+ Tregs in *Nfkb2−/−* mice. (**A**) Real-time PCR analysis of *Foxp3* expression in 5- to 7-week-old WT and *Nfkb2−/−* thymi. Data are mean ± SD for each group. (**B**) Flow cytometry analysis of intracellular *Foxp3* expression in CD4+CD8− T cells from thymus and spleen. Numbers represent the percentages within the indicated regions.

were depleted of hematopoietic cells by incubation with 2′-deoxyguanosine for 6 days and then grafted under the kidney capsules of nude mice, creating *Nfkb2−/−*→nude mice and WT→nude mice, respectively. Twelve weeks after engraftment, both *Nfkb2−/−* and WT thymi were well developed and functioned, containing approximately equal numbers of thymocytes (Figure 5A) with similar double negative (DN), double positive (DP), and single positive (SP) subset distribution (Figure 5B). Real-time PCR of *Nfkb2−/−* and WT total donor thymi found significantly reduced *Aire* and *Ins1* expression in *Nfkb2−/−* relative to WT thymi (Figure 5C). We analyzed peripheral organs including the liver, lung, pancreas, and salivary gland to determine the extent of peripheral autoimmune infiltration. While no infiltration was seen in WT→nude mice, significant infiltration was observed in nearly all *Nfkb2−/−*→nude mice (Figure 5D). Immunostaining of *Rag1−/−* tissue sections with serum from the recipient mice revealed significant autoantibod-

ies against stomach and salivary gland in the sera of *Nfkb2−/−*→ nude mice but not WT→nude mice (Figure 5E). Only 1 WT→nude mouse showed weakly positive staining, but 3 of the 4 *Nfkb2−/−*→ nude mice showed strong autoantibody reaction. These data indicate that NF-κB2 deficiency in the thymic stroma is sufficient to result in a breakdown in self tolerance.

LTβR, but not TNF receptor, is essential and sufficient for NF-κB2–mediated Aire expression. NF-κB2 is a critical signaling component downstream of both the LTβR and the TNF receptor (TNFR). TNFR-deficient and *Nfkb2−/−* mice share identical defects in splenic architecture, in addition to lacking Peyer's patches, B cell follicles, and follicular DC clusters (32, 33). LTβR-deficient mice similarly share these defects but have others in addition, for example, absence of T cell/B cell segregation and lymph node aplasia. To determine whether NF-κB2 mediates LTβR- or TNFR-dependent *Aire* expression, we treated 4- to 6-week-old WT or *Nfkb2−/−* mice intraperitoneally with agonistic anti-LTβR
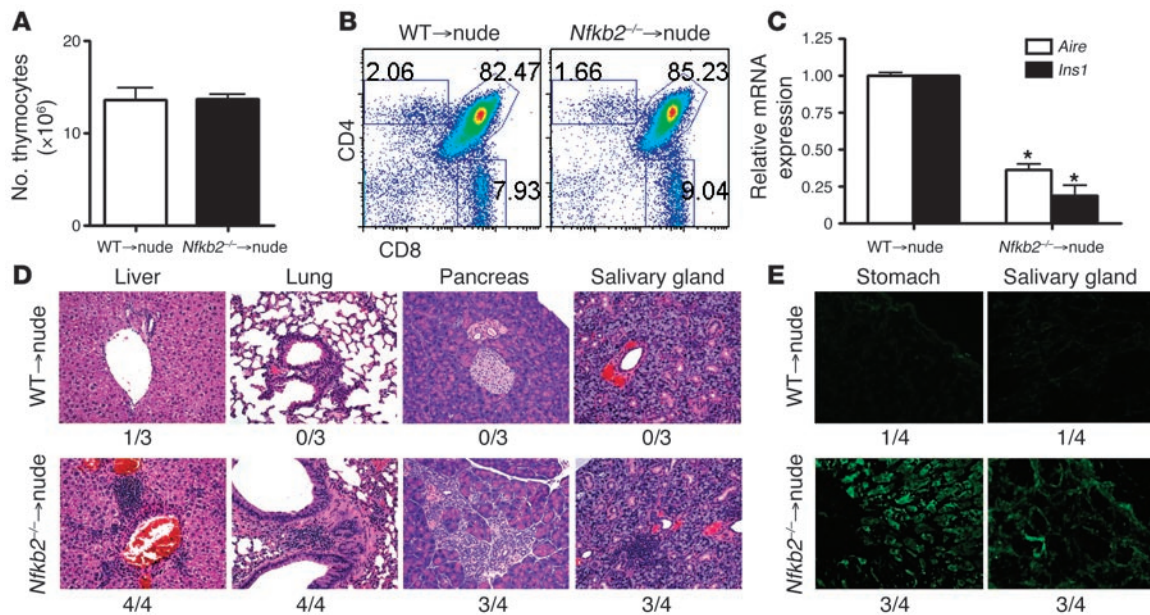

Figure 5
Nfkb2−/− thymic stroma are sufficient to induce autoimmunity in thymi-grafted nude mice. (**A** and **B**) Thymic reconstitution was analyzed by counting total cell number and flow cytometry. Numbers represent the percentages within the indicated regions. (**C**) Real-time PCR analysis of *Aire* and *Ins1* expression in grafted thymi. Values are arbitrary units normalized to *Gapdh*. Data are mean ± SD for each group. *P < 0.05 versus WT. (**D**) H&E staining of livers, lungs, pancreata, and salivary glands from nude mice grafted with WT or *Nfkb2−/−* thymic stroma 12 weeks after thymi grafting. The incidence of infiltration in the specific organs is indicated. (**E**) Immunofluorescence staining of *Rag1−/−* tissue sections to test the autoantibodies from the thymi-grafted nude mice. The incidence of infiltration in the specific organs is indicated.
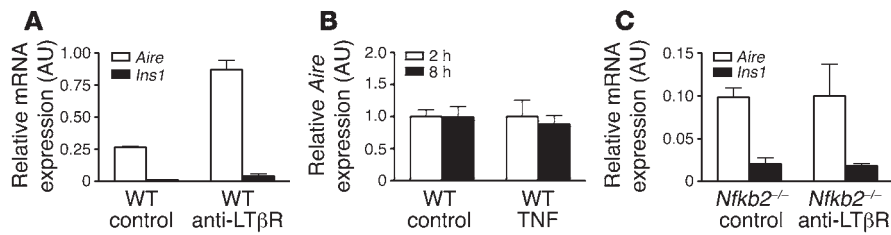
Figure 6
LTβR, not TNFR, is upstream of NF-κB2–mediated thymic *Aire* gene expression. (**A**–**C**) LTβR agonist antibody (3C8) (**A** and **C**) or recombinant TNF (**B**) was used to treat 4- to 6-week-old WT (**A** and **B**) or *Nfkb2*−/− (**C**) mice. RNA was isolated from the thymus after 6 hours (for 3C8 treatment) or 2 or 8 hours (for 1 μg TNF treatment). Real-time PCR was used to detect *Aire* and *Ins1* expression. Values are arbitrary units normalized to *Gapdh*. Data (mean ± SD for each group) are representative of 3 independent experiments.

antibody or recombinant TNF. Total thymic *Aire* expression was evaluated by real-time PCR to assay whether the absence of NF-κB2 disrupts the induction of *Aire* by these ligands. We found that 6 hours after treatment with anti-LTβR, *Aire* expression was significantly increased in WT mice (Figure 6A). At the same time, regardless of the dose (1 or 2 μg) and duration (2, 4, or 8 hours), recombinant TNF failed to induce *Aire* expression in WT mice (Figure 6B and data not shown). This is also consistent with our finding that *Aire* expression was normal in both *Tnfr*−/− and *Tnf*−/− thymi (data not shown). In *Nfkb2*−/− mice, the induction of *Aire* expression in response to agonistic anti-LTβR was largely abolished (Figure 6C). Taken together, these findings indicate that NF-κB2 regulated by LTβR is necessary for transcriptional control of thymic *Aire* gene expression.

Discussion

Disrupted thymic *Aire* expression can be the result of either impaired mTEC development and/or organization or defective transcriptional regulation. Impaired thymic *Aire* expression has been reported for NIK[aly/aly] and TRAF6-deficient mice (5, 6), though it remains unclear whether this is due to impaired mTEC development or defective *Aire* transcription. Both NIK[aly/aly] and TRAF6-deficient mice have significantly disorganized thymic medulla and an absence in the UEA-1+ subpopulation of mTECs (5, 6). While we have recently described the critical role of LTβR signaling for optimal *Aire* gene expression (7), the signaling events downstream of the LTβR remain poorly characterized. LTβR uses 2 prominent signaling pathways, namely, the canonical p50-RelA pathway and the noncanonical p52-RelB pathway (34). In contrast to *Ltbr*−/− and NIK[aly/aly] mice, *Nfkb2*−/− mice have much milder architectural changes in the spleen, retain almost all lymph nodes, and display normal thymic architecture (13, 14). Our recent study suggests that p50-RelB and p52-RelA may also play a role for the development and organization of lymphoid structures (15). Therefore, the NF-κB pathway that is responsible for LTβR-mediated *Aire* expression is still unclear. The apparent conflict between a defective T cell/B cell response to foreign antigens but increased autoimmunity in *Nfkb2*−/− mice and the similarity of the autoimmune phenotypes among *Nfkb2*−/− and *Aire*−/−, *Ltbr*−/−, *Traf6*−/−, and NIK[aly/aly] mice led us to explore the role played by NF-κB2 in central tolerance. Our finding of disrupted thymic *Aire* expression in the purified mTECs from *Nfkb2*−/− mice points to the necessity of NF-κB2 in transcriptional control of *Aire* expression. Indeed, in models of thymic transplantation, deficiency in NF-κB2 on the thymic stroma was found to be sufficient to disrupt central tolerance, leading to overt autoimmunity. The slightly impaired mTEC organization and/or development probably also contributes to the breakdown of central tolerance in *Nfkb2*−/− mice. The largely undisturbed thymic architecture in *Nfkb2*−/− thymi differs significantly from that of NIK[aly/aly] thymi, suggesting that NIK may mediate pathways in addition to p52 for the organization and development of mTECs. The more severe reduction in *Aire* expression in NIK[aly/aly] thymi relative to *Nfkb2*−/− thymi could be a consequence of concomitant reduction of both mTEC population and transcriptional activation. RelB is a critical p52 binding partner, and *Relb*−/− mice present with severe autoimmunity. While *Relb*−/− mice similarly have reduced thymic *Aire* expression, this is in the context of significantly disrupted thymic architecture and absent mTECs (35, 36). It is therefore difficult to conclude whether p52-RelB complexes are required for *Aire* expression or whether the RelB defect represents a failure in development and/or organization of mTECs. Similar difficulties exist for dissecting the potential role of RelA in central tolerance, since *Rela*−/− mice are embryonic lethal (37, 38). Whether p52 pairs with RelB or other molecules for *Aire* expression remains to be determined.

CD4+CD25+ Treg generation has been reported to be reduced in NIK[aly/aly] mice (6). Although p52 is the major signaling component downstream of NIK, Treg generation defects were found in neither the thymi nor the spleens of *Nfkb2*−/− mice. The suppressive function of Tregs from *Nfkb2*−/− mice also remains comparable to their WT counterparts. In our thymic stroma transplant experiments, we evaluated *Foxp3* mRNA expression from the total transplanted thymi and similarly found no difference between WT→nude and *Nfkb2*−/−→nude mice (data not shown). This suggests that pathways downstream of NIK other than p52 are responsible for Treg generation in thymus. Although T cell–specific ablation of IκB kinase β (IKK2), which may also be regulated by NIK, leads to reduced thymic Treg generation (39), it is not likely the case for NIK[aly/aly] mice, since NIK[aly/+] mice reconstituted with NIK[aly/aly] BM did not present with signs of autoimmunity (6). Taken together, these results suggest that NIK, through a p52-independent pathway, may regulate thymic Treg generation. By generating BM chimeras we were able to determine the autoimmune defect in *Nfkb2*−/− mice originated largely in the stromal compartment. By thymus transplant experiments, we showed that the defective thymic stroma from *Nfkb2*−/− mice was sufficient for the breakdown in self tolerance. Twelve weeks following transplant, the *Nfkb2*−/−→nude autoimmune phenotype was comparable to that of 6- to 8-month-old *Nfkb2*−/− mice. This finding points to the magnitude of the thymic defect in *Nfkb2*−/− mice. The more rapid presentation of autoimmune phenotype in the *Nfkb2*−/−→nude mice may be accounted for by the more competent secondary lymphoid structure and microarchitecture in these mice relative to the *Nfkb2*−/− mice. Additionally, the peripheral stroma of *Nfkb2*−/− mice have a demonstrated defect in supporting the immune response (13, 14). Furthermore, *Nfkb2*−/− T cells themselves have activation defects (16). In the *Nfkb2*−/−→nude mice, these additional restrictions were removed. Thus the severity of the autoimmune defect in the *Nfkb2*−/− thymus may have been in part masked by the immune-modulating defects in the periphery.

These might also account for the fact that no diabetes or hyperglycemia developed in 8- to 10-month-old *Nfkb2*⁻/⁻ mice, even in the presence of severe infiltration in the pancreas.

It is interesting that chimeric *Nfkb2*⁻/⁻ mice with WT BM cells and *Nfkb2*⁻/⁻ mice did not show the exact same infiltration pattern in affected organs. Although there was significant infiltration in the pancreata and kidneys in *Nfkb2*⁻/⁻ mice, it was rarely seen in the BM chimera. This raises the possibility of a role for hematopoietic cells such as DCs in self tolerance establishment or modulation. One explanation would be if hematopoietic APCs express self antigens targeting pancreas and kidney, thereby preventing autoimmunity to these organs in the BM-chimeric mice. Since none of the 4 TSAs we chose was detectable in thymic DCs, this hypothesis regarding central tolerance remains to be tested in future studies. However, we readily found *Ins1* and *Ins2* expression in peripheral splenic DCs and a dramatic reduction of both in *Nfkb2*⁻/⁻ mice. This might lead to impaired peripheral tolerance in *Nfkb2*⁻/⁻ mice (25). Besides self antigen expression and presentation, DCs have also been shown to play critical roles in maintaining peripheral tolerance (40–42). NF-κB2 was previously reported as a negative regulator of DC function (43). DCs lacking NF-κB2 have dramatically enhanced RelB activity, which is associated with increased MHC class II and costimulatory molecule expression and an enhanced ability to induce CD4⁺ T cell responses. This also implies a role of NF-κB2 in peripheral tolerance maintenance. The delineation and definition of the role of *Nfkb2*⁻/⁻ DCs for self tolerance remain to be explored in the future.

Our study defines the role of NF-κB2 in regulating thymic *Aire* expression and thereby contributing to the maintenance of central tolerance. Our finding also clarifies that the p52 pathway is a primary pathway downstream of the LTβR responsible for Aire-dependent central tolerance. The understanding of how the *Aire* gene is regulated may provide better diagnostic and therapeutic possibilities in the future treatment of autoimmune diseases.

Methods

Mice. *Nfkb1*⁻/⁻ and *Nfkb2*⁻/⁻ mice were previously described (14, 44). *Aire*⁻/⁻ mice were generated with a mixed genetic background as described previously (45) and backcrossed to C57BL/6 for at least 6 generations in the lab of Y.-X. Fu. C57BL/6 mice and *Foxn1*ⁿᵘ mice (nude mice) were purchased from The Jackson Laboratory. Mice were maintained in a specific pathogen–free facility. Animal care and experiments were performed in accordance with institutional and NIH guidelines and were approved by the animal use committee at the University of Chicago.

Histopathology. Tissues for histological examination were fixed in 10% buffered formalin and embedded in paraffin. Four- to five-micron sections were obtained from the paraffin blocks and stained using H&E stain methods. All sections were then examined by a pathologist in a blinded fashion. NIH ImageJ version 1.34s software (http://rsb.info.nih.gov/ij/) was used to calculate the thymic cortical and medullary areas.

Immunofluorescence staining. Six-micron frozen sections were fixed in acetone at 4°C for 10 minutes, rehydrated in PBS/saponin (0.1%), and blocked with goat serum (5%) or BSA (1%) in PBS at room temperature for 1 hour. For autoantibody detection, sera were diluted 1:60 and incubated overnight at 4°C. Anti-mouse IgG(H+L)–FITC (CALTAG Laboratories) was used for visualization. For thymus staining, antibodies G8.8 (BD Biosciences — Pharmingen), UEA-1–bio (Sigma-Aldrich), and polyclonal rabbit anti-Aire (gift from P. Peterson, Molecular Pathology, University of Tartu, Tartu, Estonia) were incubated with sections at 4°C overnight and detected with appropriate fluorescence reagents. NIH ImageJ version 1.34s software was used to calculate the G8.8⁺ and UEA-1⁺ area.

Flow cytometry analysis. Single-cell suspensions from the lung were stained with anti-CD4 (GK1.5), anti-CD8 (53-6.7), anti-CD44 (IM7), and anti-CD69 (H1.2F3) monoclonal antibodies (BD Biosciences — Pharmingen) in cold PBS containing 0.2% BSA and 0.09% sodium azide. Before staining, the cells were preincubated with anti–FcγIII/II receptor (2.4G2; BD Biosciences — Pharmingen). Foxp3 intracellular staining was carried out using Mouse Regulatory T cell Staining Kit according to the manufacturer's instructions (eBioscience). Stained cells were analyzed on FACSCalibur (BD Biosciences). For mTEC sorting, the thymus was digested, and mTECs were enriched by incontinuous Percoll gradient centrifuge as described previously (3). Enriched mTECs were stained with anti–Ep-CAM (G8.8), anti-CD45.2 (104), anti-CD80 (16-10A1), and appropriate secondary fluorescence reagents (BD Biosciences — Pharmingen). The CD45.2⁻G8.8⁺CD80⁺ population was sorted on FACSAria (BD Biosciences). For thymic DC sorting, after thymic digestion, DCs were stained with anti-CD11c (HL3) and anti-I-A/I-E (M5/114.15.2) (BD Biosciences — Pharmingen). DCs were sorted as the CD11c⁺I-A⁺ population. For splenic DC isolation, CD11c (N418) Micro-Beads (Miltenyi Biotec) was used following the manufacturer's protocol.

Real-time PCR. Real-time PCR was carried out on cDNA prepared from DNase I–treated RNA extracted from whole thymus, purified mTECs, or DCs. The primers and probes used were as follows: *Aire* forward, 5′-CCAGT-GAGCCCCAGGTTAAC-3′; reverse, 5′-GACAGCCGTCACAACAGATGA-3′; probe, 5′-FAM-TCACCTCCGTCGTGGCACACG-TAMRA-3′; *Ins1* forward, 5′-CTTCAGACCTTGGCGTTGGA-3′; reverse, 5′-ATGCTGGTGCAGCACT-GATC-3′; probe, 5′-FAM-CCCGGCAGAAGCGTGGCATT-TAMRA-3′; *Ins2* forward, 5′-GACCCACAAGTGGCACAA-3′; reverse, 5′-ATCTACAAT-GCCACGCTTCTG-3′; probe, 5′-FAM-CCCGGGAGCAGGTGACCTT-TAMRA-3′; *Csna* forward, 5′-TTTGCTATGCCCAGACTTCA-3′; reverse, 5′-TTTCCTCACTGCTGCTATGC-3′; probe, 5′-FAM-TGCAGTTAG-CAGTCAAACTCAGCAACA-TAMRA-3′; *Sp1* forward, 5′-GTGTTGCTTG-GTGTTTCCAC-3′; reverse, 5′-GCAGAATCAGCAGTTCCAGA-3′; probe, 5′-FAM-TGCCAGGACCCGGAGACAAA-TAMRA-3′; *Gapdh* forward, 5′-TTCACCACCATGGAGAAGGC-3′; reverse, 5′-GGCATGGACTGTGGTCAT-GA-3′; probe, 5′-FAM-TGCATCCTGCACCACCAACTGCTTAG-TAMRA-3′; and *Krt14* forward, 5′-TGGGTGGAGACGTCAATGTG-3′; reverse, 5′-ATCTCGTTCAGGATGCGGC-3′; probe, 5′-FAM-ACGCCGCCCCTGGT-GTGG-TAMRA-3′. Reactions were run on the 7300 Real-Time PCR System (Applied Biosystems) in a final volume of 25 μl with 900 nM of the forward and reverse primers and 200 nM of the probe using 2× TaqMan Universal PCR Master Mix (Applied Biosystems) containing AmpliTaq Gold DNA Polymerase. Cycling conditions were a single denaturing step at 95°C for 15 minutes followed by 45 cycles of 94°C for 15 seconds and 60°C for 1 minute. Analysis of *Aire*, *Ins1*, *Ins2*, *Csna*, *Sp1*, *Gapdh*, and *Krt14* gene expression was performed with a concurrently run standard curve, then normalized to sample *Gapdh* or *Krt14* levels. The standard curves had r^2 values of at least 0.99.

In vivo stimulation. WT and *Nfkb2*⁻/⁻ mice received intraperitoneal injections of 50 μg agonistic LTβR Ab (3C8), 1 or 2 μg recombinant TNF (Chemicon International), or rat-IgG isotype control in PBS. RNA from thymi was collected at the time points indicated in the Results. Real-time PCR was carried out on cDNA prepared from DNase I–treated RNA.

Autoantibody ELISA. For the detection of insulin autoantibodies, insulin was coated at 2 U/ml, and goat anti-mouse IgG-AP and IgM-AP (SouthernBiotech) were used as detecting antibodies. Antibody levels are shown in arbitrary units calculated from a standard curve.

BM reconstitution. Mice were lethally irradiated with 10 Gy and adoptively transferred i.v. with 3 × 10⁶ BM cells. Bactrim was added to the drinking water for 3 weeks following irradiation. Tissue sections from the mice were analyzed 12 weeks after transfer.

Thymic transplantation. Thymi were isolated from newborn *Nfkb2*⁻/⁻ or WT mice and cultured in 1.35 mM 2′-deoxyguanosine (Sigma-Aldrich) for 6–8

days to deplete BM-derived cells. Thymi were then transplanted under the kidney capsule of 6-week-old nude mice. Whole blood was collected 12 weeks after transplantation. Thymus recovery was determined by staining of thymocytes with anti-CD4 and anti-CD8 as described above. Serum was used to stain *Rag1*−/− tissue sections by immunofluorescence as described above.

Statistics. Statistical significance was determined by 2-tailed Student's *t* test. *P* values less than 0.05 were considered statistically significant. Unless otherwise specified, all data are presented as mean ± SD.

1. Derbinski, J., Schulte, A., Kyewski, B., and Klein, L. 2001. Promiscuous gene expression in medullary thymic epithelial cells mirrors the peripheral self. *Nat. Immunol.* **2**:1032–1039.
2. Gotter, J., Brors, B., Hergenhahn, M., and Kyewski, B. 2004. Medullary epithelial cells of the human thymus express a highly diverse selection of tissue-specific genes colocalized in chromosomal clusters. *J. Exp. Med.* **199**:155–166.
3. Anderson, M.S., et al. 2002. Projection of an immunological self shadow within the thymus by the aire protein. *Science.* **298**:1395–1401.
4. Liston, A., Lesage, S., Wilson, J., Peltonen, L., and Goodnow, C.C. 2003. Aire regulates negative selection of organ-specific T cells. *Nat. Immunol.* **4**:350–354.
5. Akiyama, T., et al. 2005. Dependence of self-tolerance on TRAF6-directed development of thymic stroma. *Science.* **308**:248–251.
6. Kajiura, F., et al. 2004. NF-kappa B-inducing kinase establishes self-tolerance in a thymic stroma-dependent manner. *J. Immunol.* **172**:2067–2075.
7. Chin, R.K., et al. 2003. Lymphotoxin pathway directs thymic Aire expression. *Nat. Immunol.* **4**:1121–1127.
8. Boehm, T., Scheu, S., Pfeffer, K., and Bleul, C.C. 2003. Thymic medullary epithelial cell differentiation, thymocyte emigration, and the control of autoimmunity require lympho-epithelial cross talk via LTbetaR. *J. Exp. Med.* **198**:757–769.
9. Futterer, A., Mink, K., Luz, A., Kosco-Vilbois, M.H., and Pfeffer, K. 1998. The lymphotoxin beta receptor controls organogenesis and affinity maturation in peripheral lymphoid tissues. *Immunity.* **9**:59–70.
10. Yin, L., et al. 2001. Defective lymphotoxin-beta receptor-induced NF-kappaB transcriptional activity in NIK-deficient mice. *Science.* **291**:2162–2165.
11. Miyawaki, S., et al. 1994. A new mutation, aly, that induces a generalized lack of lymph nodes accompanied by immunodeficiency in mice. *Eur. J. Immunol.* **24**:429–434.
12. Shinkura, R., et al. 1999. Alymphoplasia is caused by a point mutation in the mouse gene encoding Nf-kappa b-inducing kinase. *Nat. Genet.* **22**:74–77.
13. Caamano, J.H., et al. 1998. Nuclear factor (NF)-kappa B2 (p100/p52) is required for normal splenic microarchitecture and B cell-mediated immune responses. *J. Exp. Med.* **187**:185–196.
14. Franzoso, G., et al. 1998. Mice deficient in nuclear factor (NF)-kappa B/p52 present with defects in humoral responses, germinal center reactions, and splenic microarchitecture. *J. Exp. Med.* **187**:147–159.
15. Lo, J.C., et al. 2006. Coordination between NF-kappaB family members p50 and p52 is essential for mediating LTbetaR signals in the development and organization of secondary lymphoid tissues. *Blood.* **107**:1048–1055.
16. Caamano, J., et al. 2000. Identification of a role for NF-kappa B2 in the regulation of apoptosis and in maintenance of T cell-mediated immunity to Toxoplasma gondii. *J. Immunol.* **165**:5720–5728.
17. Farr, A., Nelson, A., Truex, J., and Hosier, S. 1991. Epithelial heterogeneity in the murine thymus: a cell surface glycoprotein expressed by subcapsular and medullary epithelium. *J. Histochem. Cytochem.* **39**:645–653.
18. Farr, A.G., and Anderson, S.K. 1985. Epithelial heterogeneity in the murine thymus: fucose-specific lectins bind medullary epithelial cells. *J. Immunol.* **134**:2971–2977.
19. Derbinski, J., et al. 2005. Promiscuous gene expression in thymic epithelial cells is regulated at multiple levels. *J. Exp. Med.* **202**:33–45.
20. Liston, A., et al. 2004. Gene dosage--limiting role of Aire in thymic expression, clonal deletion, and organ-specific autoimmunity. *J. Exp. Med.* **200**:1015–1026.
21. Klug, D.B., et al. 1998. Interdependence of cortical thymic epithelial cell differentiation and T-lineage commitment. *Proc. Natl. Acad. Sci. U. S. A.* **95**:11822–11827.
22. Ramsey, C., et al. 2006. Increased antigen presenting cell-mediated T cell activation in mice and patients without the autoimmune regulator. *Eur. J. Immunol.* **36**:305–317.
23. Anderson, M.S., et al. 2005. The cellular mechanism of Aire control of T cell tolerance. *Immunity.* **23**:227–239.
24. Garcia, C.A., et al. 2005. Dendritic cells in human thymus and periphery display a proinsulin epitope in a transcription-dependent, capture-independent fashion. *J. Immunol.* **175**:2111–2122.
25. Zheng, X., Yin, L., Liu, Y., and Zheng, P. 2004. Expression of tissue-specific autoantigens in the hematopoietic cells leads to activation-induced cell death of autoreactive T cells in the secondary lymphoid organs. *Eur. J. Immunol.* **34**:3126–3134.
26. Throsby, M., et al. 1998. Pancreatic hormone expression in the murine thymus: localization in dendritic cells and macrophages. *Endocrinology.* **139**:2399–2406.
27. Khattri, R., Cox, T., Yasayko, S.A., and Ramsdell, F. 2003. An essential role for Scurfin in CD4+CD25+ T regulatory cells. *Nat. Immunol.* **4**:337–342.
28. Hori, S., Nomura, T., and Sakaguchi, S. 2003. Control of regulatory T cell development by the transcription factor Foxp3. *Science.* **299**:1057–1061.
29. Fontenot, J.D., Gavin, M.A., and Rudensky, A.Y. 2003. Foxp3 programs the development and function of CD4+CD25+ regulatory T cells. *Nat. Immunol.* **4**:330–336.
30. Jordan, M.S., et al. 2001. Thymic selection of CD4+CD25+ regulatory T cells induced by an agonist self-peptide. *Nat. Immunol.* **2**:301–306.
31. Lerman, M.A., Larkin, J., 3rd, Cozzo, C., Jordan, M.S., and Caton, A.J. 2004. CD4+ CD25+ regulatory T cell repertoire formation in response to varying expression of a neo-self-antigen. *J. Immunol.* **173**:236–244.
32. Weih, F., and Caamano, J. 2003. Regulation of secondary lymphoid organ development by the nuclear factor-kappaB signal transduction pathway. *Immunol. Rev.* **195**:91–105.
33. Fu, Y.X., and Chaplin, D.D. 1999. Development and maturation of secondary lymphoid tissues. *Annu. Rev. Immunol.* **17**:399–433.
34. Dejardin, E., et al. 2002. The lymphotoxin-beta receptor induces different patterns of gene expression via two NF-kappaB pathways. *Immunity.* **17**:525–535.
35. Zuklys, S., et al. 2000. Normal thymic architecture and negative selection are associated with Aire expression, the gene defective in the autoimmune-polyendocrinopathy-candidiasis-ectodermal dystrophy (APECED). *J. Immunol.* **165**:1976–1983.
36. Heino, M., et al. 2000. RNA and protein expression of the murine autoimmune regulator gene (Aire) in normal, RelB-deficient and in NOD mouse. *Eur. J. Immunol.* **30**:1884–1893.
37. Beg, A.A., Sha, W.C., Bronson, R.T., Ghosh, S., and Baltimore, D. 1995. Embryonic lethality and liver degeneration in mice lacking the RelA component of NF-kappa B. *Nature.* **376**:167–170.
38. Doi, T.S., Takahashi, T., Taguchi, O., Azuma, T., and Obata, Y. 1997. NF-kappa B RelA-deficient lymphocytes: normal development of T cells and B cells, impaired production of IgA and IgG1 and reduced proliferative responses. *J. Exp. Med.* **185**:953–961.
39. Schmidt-Supprian, M., et al. 2003. Mature T cells depend on signaling through the IKK complex. *Immunity.* **19**:377–389.
40. Steinman, R.M., Hawiger, D., and Nussenzweig, M.C. 2003. Tolerogenic dendritic cells. *Annu. Rev. Immunol.* **21**:685–711.
41. Moser, M. 2003. Dendritic cells in immunity and tolerance-do they display opposite functions? *Immunity.* **19**:5–8.
42. Chen, M., et al. 2006. Dendritic cell apoptosis in the maintenance of immune tolerance. *Science.* **311**:1160–1164.
43. Speirs, K., Lieberman, L., Caamano, J., Hunter, C.A., and Scott, P. 2004. Cutting edge: NF-kappa B2 is a negative regulator of dendritic cell function. *J. Immunol.* **172**:752–756.
44. Sha, W.C., Liou, H.C., Tuomanen, E.I., and Baltimore, D. 1995. Targeted disruption of the p50 subunit of NF-kappa B leads to multifocal defects in immune responses. *Cell.* **80**:321–330.
45. Ramsey, C., et al. 2002. Aire deficient mice develop multiple features of APECED phenotype and show altered immune response. *Hum. Mol. Genet.* **11**:397–409.